Electron Capture and Ionization of Pb Ions at 33 TeV

H. F. Krause,[1] C. R. Vane,[1] S. Datz,[1] P. Grafström,[2] H. Knudsen,[3] C. Scheidenberger,[4] and R. H. Schuch[5]
[1]*Physics Division, Oak Ridge National Laboratory, P.O. Box 2008, Oak Ridge, Tennessee 37831-6377*
[2]*CERN SPS/SL Division, CH-1211, Geneva 23, Switzerland*
[3]*Institute of Physics, Aarhus University, DK-8000, Aarhus C, Denmark*
[4]*Gesellschaft für Schwerionenforschung mbh, Planckstrasse 1, D-64291, Darmstadt, Germany*
[5]*Atomic Physics Department, Stockholm University, Frescativägen 24, S-104 05, Stockholm 50, Sweden*
(Received 8 September 1997)

We have measured the total cross sections for electron capture by bare Pb^{82+} ions and ionization of hydrogenlike Pb^{81+} ions at 33 TeV (160 GeV/A, $\gamma = 168$) in solid targets of Be, C, Al, Cu, Sn, and Au. The total capture cross sections are dominated by electron capture from pair production and are compared with theoretical calculations. The $1s$ ionization cross sections obtained are significantly smaller than those predicted by Anholt and Becker [Phys. Rev. A **36**, 4628 (1987)]. The Pb radiative lifetimes extended by $\gamma = 168$ have a strong effect on the survival probability of excited states against ionization in high-Z solid targets. [S0031-9007(97)05213-7]

PACS numbers: 34.50.Fa, 34.80.Lx

Interactions involving high-Z ions in the ultrarelativistic regime (>10 GeV/amu), where the relevant physics is best described in terms of the Lorentz factor γ, are currently a frontier in high-energy atomic collision physics [1]. A theoretical description of electron capture and ionization processes has been challenging in this regime because the interaction of high-Z projectile and target species (where $Z\alpha \sim 0.5$) is strong enough at small impact parameters and large γ to potentially invalidate perturbation treatments. Numerous methods for treating these processes using quantum electrodynamics (QED) in the ultrarelativistic regime now exist [1–10].

An ultrarelativistic ion can capture an electron via three mechanisms: (i) radiative electron capture (REC), (ii) nonradiative capture (NRC), and (iii) electron capture via e^+e^- pair production (ECPP), in which the e^+e^- pair is produced by the intense electromagnetic pulse that arises when the projectile ion passes near a target nucleus. Capture cross sections σ_{REC}, σ_{NRC}, and σ_{ECPP} scale roughly as $\sim Z_t/\gamma$, $\sim Z_t^5/\gamma$, and $\sim Z_t^2 \ln\gamma$, respectively, where Z_t is the target atomic number [2]. Each process has approximately the same dependence on the projectile atomic number, i.e., Z_p^5. The REC and NRC mechanisms, which dominate below the ultrarelativistic regime [11–13], become insignificant compared to ECPP when $\gamma > 100$ even for high Z_t. We report the first high-energy measurements ($\gamma = 168$) where σ_{ECPP} dominates the capture cross sections of competing mechanisms. Ionization cross sections are several orders of magnitude larger than capture, and our measurements test theory at the highest energy reported to date [2,10].

The development of new relativistic ion colliders such as the Relativistic Heavy-Ion Collider at Brookhaven National Laboratory or the Large Hadron Collider at CERN [2,8,14] requires knowledge of the capture cross sections at high enough γ so that beam lifetimes can be accurately predicted. The cross section for the ECPP process is of practical interest to collider designers because the lower charge-state projectiles produced are lost from the beam circulating in a ring. A significant loss rate of these ions by ECPP and also by nuclear loss processes decreases the ion storage time. These machines will operate at an effective γ of 2.3×10^4 and 1.7×10^7, respectively. For γ above ~100, the $\ln\gamma$ scaling will be valid and $\sigma_{\mathrm{ECPP}} = A \ln\gamma + B$, where A and B are predicted to be [4] independent of $1/\gamma$. Total electron capture and loss measurements were reported recently by Claytor *et al.* [12] for $\gamma = 12.6$-Au ions, but the ECPP mechanism is not prominent at this low γ, and $\ln\gamma$ scaling is not expected to be valid.

We report total capture and ionization cross sections measured using the Pb beam at the CERN Super Proton Synchrotron (SPS). In the "capture experiment," Fig. 1, collimated $^{208}Pb^{82+}$ ions were mass and charge-state selected at the first magnetic bend before impinging on a thin solid target located ~100 m downstream. The second bend and collimator at ~100 m beyond the target of the beam line was set to transmit all $^{208}Pb^{81+}$ ions leaving the target. The ion intensity at the end of the

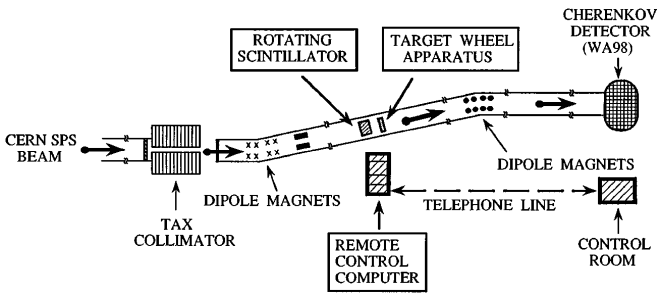

FIG. 1. Simplified diagram of the experimental setup.

 0031-9007/98/80(6)/1190(4)$15.00

0.8-Km beam line was measured using the coincidence signal from fast Cherenkov detectors [15]. The same setup was used in the "ionization experiment" except that the full beam line was tuned to transmit $^{208}Pb^{81+}$ ions, and we measured the Pb^{81+} ions which survived using the same targets [16]. The incident $Pb^{81+}(1s)$ ions were formed by electron capture in the SPS beam line prior to entering our vacuum line ($\sim 10^{-3} \times Pb^{82+}$ intensity). The beam line was evacuated to a pressure of ~ 10 mTorr between the (TAX) beam collimator and the Cherenkov detectors. At this pressure, the column gas density in the beam line is low enough to limit collisional loss of the Pb^{81+} ions to less than $\sim 1\%$ between the target and Cherenkov detectors.

Experimental data illustrating growth in the Pb^{81+} ion fraction versus Au target thickness (capture experiment) are shown in Fig. 2(a). Data illustrating the loss of the Pb^{81+} ion fraction versus Au target thickness (ionization experiment), using the same targets, are shown in Fig. 2(b). The data were used to determine the effective cross sections for capture (σ_c) and loss (σ_i) processes. Because σ_c is orders of magnitude smaller than σ_i, only two charge states (Pb^{81+} and Pb^{82+}) need to be considered and the coupled differential equations reduce to a simple analytical form. The cross sections were determined for capture by Pb^{82+} and ionization of Pb^{81+} by fitting data obtained in the capture experiment [Fig. 2(a)] using the equation

$$F(81) = F_{\mathrm{eq}}\{1 - \exp[-(\sigma_c + \sigma_i)t]\}\exp[-\sigma_n t], \quad (1)$$

where $F(81)$ is the fraction of Pb^{81+} ions, σ_c is the total capture cross section (cm^2), σ_i is the total ionization cross section, σ_n is the total cross section for beam loss by nuclear reactions (cm^2), t is the target thickness ($atom/cm^2$), and $F_{\mathrm{eq}} = [\sigma_c/(\sigma_c + \sigma_i)]$ is the equilibrium 81+ charge fraction. The values σ_n used throughout for Be, C, Al, Cu, Sn, and Au are 4.0, 4.5, 7.4, 15.2, 31.0, and 64.0 b, respectively [17].

In the ionization experiment [Fig. 2(b)], the surviving fraction of Pb^{81+} ions is given by

$$F(81) = \{[1 - F_{\mathrm{eq}}]\exp[-(\sigma_c + \sigma_i)t] + F_{\mathrm{eq}}\} \times \exp[-\sigma_n t]. \quad (2)$$

The nuclear loss term in Eqs. (1) and (2) was an insignificant correction except for Be and C (9% and 3%, respectively, for the thickest target). Here the slope of the exponential fit to the survival charge fraction corrected for nuclear loss, shown in Fig. 2(b), yields $\sigma_i + \sigma_c$ directly.

The cross sections for each target species are shown in Table I. The overall uncertainty in each value of about $\pm 10\%$ includes the fitting error and estimated uncertainties for target thickness ($\pm 2\%$) and inhomogeneity ($\pm 5\%$). Each measured total capture cross section (σ_c) is the sum of three processes, $\sigma_c = \sigma_{\mathrm{ECPP}} + \sigma_{\mathrm{REC}} + \sigma_{\mathrm{NRC}}$. Subtracting the calculated values [2] of σ_{REC} and σ_{NRC} yields the σ_{ECPP} values listed in Table I. Three theoretical values for σ_{ECPP}, the dominant contribution to the total, are available. The perturbative estimate of Anholt and Becker [2] (with screening) is given in tables for each projectile and target. The nonperturbative calculation of Bottcher and Strayer [3], obtained specifically for capture to $1s$ at $\gamma = 168$ for the Pb-Au system by solving the time-dependent Dirac equation, yielded $\sigma_{\mathrm{ECPP}}(1s) = 50$ b. The nonperturbative calculations of Baltz *et al.* [8] yielded $\sigma_{\mathrm{ECPP}}(1s) = 46$ b for the Pb-Au system at $\gamma = 168$. In the comparisons to be discussed, the σ_{ECPP} have been scaled to each Z_t measured according to $[Z_t^2 + Z_t]$, as recommended by Anholt and Becker.

Comparisons of experimental and theoretical σ_{ECPP} are presented as functions of Z_t in Fig. 3(a). The cross sections are normalized to results of the calculations by Baltz *et al.*, with the target dependence scaled as $Z_t^2 + Z_t$. We note exceptionally good agreement between experiment and calculations by Baltz *et al.* and Anholt and Becker for heavy targets (Sn and Au), while measured

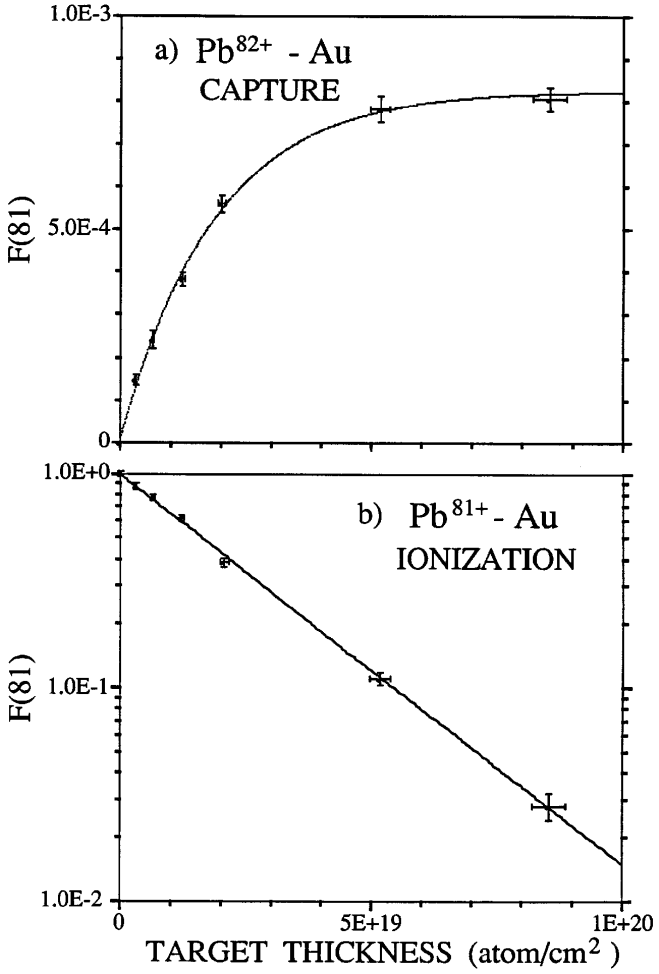

FIG. 2. (a) Fraction of one-electron Pb^{81+} ions versus Au target thickness measured in the capture experiment. The solid curve is the growth curve [Eq. (1)] calculated using the cross sections σ_c and σ_i obtained via a least squares fitting procedure. (b) Log plot of the surviving fraction of $Pb^{81+}(1s)$ ions versus Au target thickness measured in the ionization experiment. The least squares fit to the data is shown.

TABLE I. Capture and ionization cross sections in barns and kilobarns, respectively. The total capture (σ_c) and ionization (σ_i) cross sections were obtained directly from experimental data; σ_{ECPP} is derived from σ_c (see text). The estimated accuracy of measured cross sections is $\pm 10\%$.

			Capture expt. (82+ in)		Ion. expt. (81+ in)	Ion. theory [2]
Target	Z_t	σ_{ECPP} (b)	σ_c (b)	σ_i (kb)	σ_i (kb)	$\sigma_i(1s)$ (kb)
Be	4	0.18	0.23	0.15	0.14	0.24
C	6	0.36	0.44	0.31	0.31	0.49
Al	13	1.5	1.6	1.4	1.3	2.0
Cu	29	6.8	7.2	8.0	6.9	9.0
Sn	50	18	19.2	21	15	25
Au	79	43	44.3	53	42	60

cross sections exceed theory by as much as ~20% for light targets (Be and C). The observed deviations from simple $\sim(Z_t^2 + Z_t)$ scaling of σ_{ECPP} for low Z_t are interpreted to arise from enhanced survival of excited states for light targets.

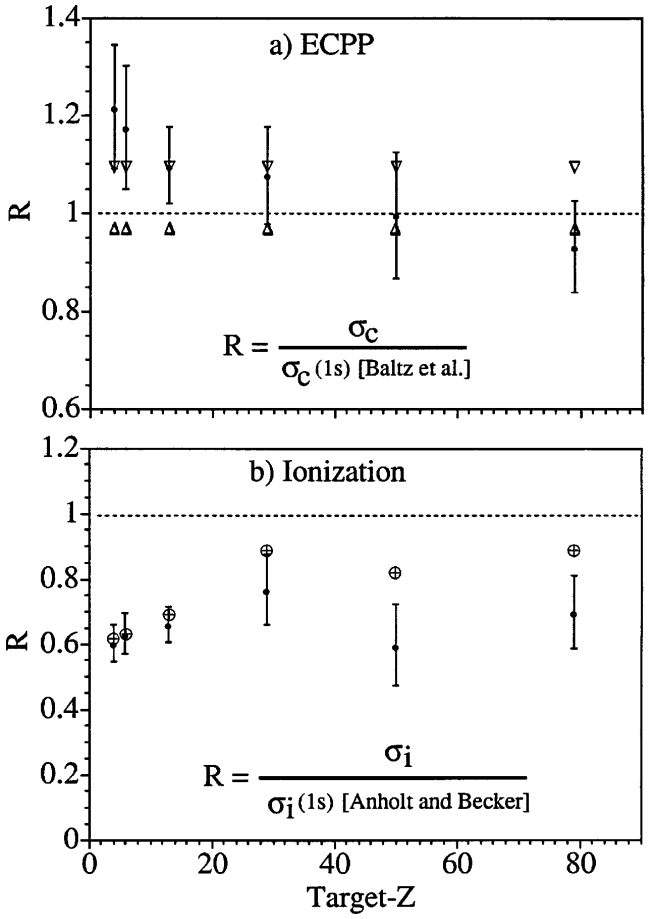

FIG. 3. Comparison of experimental and theoretical cross sections. (a) The measured σ_{ECPP} (●) and theoretical results of Bottcher and Strayer (▽) and Anholt and Becker (△) are normalized to the recent $\sigma_{\mathrm{ECPP}}(1s)$ results of Baltz ($R = 1$). (b) Ionization cross sections obtained in the capture ⊕ and ionization (●) experiments are normalized to the predicted $1s$ cross sections of Anholt and Becker ($R = 1$).

Survival of one-electron ions formed in excited states is markedly target dependent because of the varying strengths of competition between ionization in subsequent collisions in solid targets and radiative decay to $Pb^{81+}(1s)$, which is much more difficult to ionize. For example, the mean free path for radiative decay of $\gamma = 168$, $Pb^{81+}(2p \rightarrow 1s)$ is 2.3×10^{-4} cm [18]. In beryllium, the mean free path for ionization of $2p$ is $\sim 1.4 \times 10^{-2}$ cm (assuming that the $2p$-ionization cross section is 4 times as large as the measured $1s$-ionization cross section.) The fraction of $Pb^{81+}(2p)$ which radiatively stabilizes to $1s$ in Be is therefore ~98%. In gold, the mean free path for $2p$ ionization is only $\sim 1 \times 10^{-4}$ cm, and only ~30% of the $Pb^{81+}(2p)$ ions formed in the target survive ionization, to potentially contribute to the measured Pb^{81+} yields from which the capture cross section is derived. Thus contributions to the measured σ_{ECPP} from excited states are small for the heaviest targets. In gold, for example, if 20% of ECPP occurs to $n = 2$, and only ~30% of those events survive secondary ionization, then the Pb^{81+} yield will deviate from $\sigma_{\mathrm{ECPP}}(1s)$ by $\lesssim 6\%$.

Additional information is provided by the direct ionization measurements of primarily ground state ions in the ionization experiment. In Fig. 3(b), we compare the ionization cross sections obtained from both the growth (capture experiment) and decay curves (ionization experiment) to the theoretical values of Anholt and Becker. The experimental values are normalized to theory and the ratio R is plotted. All measured ionization experiment cross sections (lower values shown) are roughly $\frac{2}{3}$ of the $1s$-ionization cross sections predicted [2]. Baltz recently performed an exact time-dependent solution of the Dirac equation for Pb-Pb ionization at $\gamma = 168$ and found that the $1s$-ionization cross section is approximately 70% of the Anholt and Becker unscreened value [10]. With screening included [2] and scaled to a Au target, the Baltz value agrees with the σ_i measured in the ionization experiment (4.2×10^4 b).

The Anholt and Becker calculations add the Coulomb and transverse ionization transition amplitudes incoherently. It has been suggested that interferences between Coulomb and magnetic terms may significantly reduce the

ionization cross sections at sufficiently high energy. Such effects have been observed for collisional excitation at relativistic energies [19].

The capture and ionization experiments yield the same σ_i for the low Z_t (Be, C, and Al), where excited-state electrons have time between collisions to stabilize to $1s$, but as Z_t increases (Cu, Sn, and Au), the σ_i obtained from the capture experiment increasingly exceed those obtained in the ionization experiment. The effective σ_i is the sum of the ground and excited state cross sections weighted by the average fraction of each state as the ions traverse the targets. The fractional excess $[\sigma_i(\text{capture})\text{-}\sigma_i(\text{ionization})]/\sigma_i(\text{ionization})$ is roughly consistent with the fractional loss of ions that were captured into excited states and ionized inside the high-Z_t targets. The difference in this fraction for low- and high-Z_t targets again lies in the fate of excited states created in each experiment.

It is expected from calculations for photon impact pair production with capture using relativistic Coulomb scattering states [9] that excited ion states will contribute $\sim 30\%$ to the total cross sections of σ_{ECPP} when additional contributions from $2p$ and higher states are included. Similar predictions $(25 \pm 5)\%$ have been made by Baltz [8]. Assuming that the fraction of excited-state capture is target independent and that radiative stabilization to $1s$ occurs at grossly the $(2p \rightarrow 1s)$ decay rate, one can estimate the excited-state contributions to σ_{ECPP} and derive $\sigma_{\mathrm{ECPP}}(1s)$ versus Z_t. Analysis of the capture and ionization measurements together has shown that $\sim(15\text{–}20)\%$ of capture occurs through the $n = 2$ and higher states.

The equilibrium fractions $F_{\mathrm{eq}}(81+) = \sigma_c/(\sigma_c + \sigma_i)$ obtained in the capture analysis are 1.6×10^{-3}, 1.4×10^{-3}, 1.2×10^{-3}, 8.9×10^{-4}, 9.2×10^{-4}, and 8.3×10^{-4} for Be, C, Al, Cu, Sn, and Au, respectively. The values pertain only to equilibrium in solid targets where the measured σ_c is smaller due to loss of Pb^{81+} ions in excited states, and the σ_i is increased because of a small steady state population of excited states. The $F_{\mathrm{eq}}(81+)$ are expected to be larger in gas targets, especially for high-Z_t targets, where the mean free path can be made much larger than excited state decay distances in the laboratory frame.

In summary, our experiments have isolated the ECPP mechanism for capture. Our measured capture cross sections are consistent with theoretical values in low-Z_t targets if one includes a $\sim 20\%$ contribution from excited states. The capture cross sections measured for high-Z_t targets, where excited ions formed are rapidly lost to ionization inside the solid targets, agree with the theoretical cross sections for capture into the $1s$ state. Our loss cross sections are significantly lower than those predicted by Anholt and Becker, but agree with recent QED calculations of Baltz scaled to Pb-Au.

H. F. K., C. R. V., and S. D. gratefully acknowledge support by the U.S. DOE, Office of Basic Energy Sciences, Division of Chemical Sciences, under Contract No. DE-AC05-96OR22464 with Lockheed Martin Energy Research Corporation. H. K. acknowledges the support of the Danish Natural Science Research Council.

[1] For reviews of relativistic ion-atom collisions, see, for example, J. Eichler and W. E. Meyerhof, *Relativistic Atomic Collisions* (Academic Press, San Diego, 1995); R. Anholt and H. Gould, in *Advances in Atomic and Molecular Physics*, edited by D. Bates and B. Bederson (Academic Press, Orlando, 1986), pp. 315–386, and references therein.
[2] R. Anholt and U. Becker, Phys. Rev. A **36**, 4628 (1987).
[3] C. Bottcher and M. R. Strayer, Phys. Rev. Lett. **54**, 669 (1985); Phys. Rev. D **39**, 1330 (1989); (private communication).
[4] A. J. Baltz, M. J. Rhoades-Brown, and J. Weneser, Phys. Rev. A **44**, 5668 (1991); **47**, 3444 (1993); **48**, 2002 (1993); **50**, 4842 (1994).
[5] A. Aste, K. Hencken, D. Trautmann, and G. Baur, Phys. Rev. A **50**, 3980 (1994).
[6] M. C. Güclü, J. C. Wells, A. S. Umar, M. R. Strayer, and D. J. Erust, Phys. Rev. A **51**, 1836 (1995).
[7] K. Momberger, A. Belkacem, and A. H. Sørensen, Phys. Rev. A **53**, 1605 (1996).
[8] A. J. Baltz, M. J. Rhoades-Brown, and J. Weneser, Phys. Rev. E **54**, 4233 (1996).
[9] C. K. Agger and A. H. Sørensen, Phys. Rev. A **55**, 402 (1997).
[10] Calculation of ionization cross sections, A. J. Baltz (private communication).
[11] A. Westphal and Y. D. He, Phys. Rev. Lett. **71**, 1160 (1993).
[12] N. Claytor, A. Belkacem, T. Dinneen, B. Feinberg, and Harvey Gould, Phys. Rev. A **55**, R842 (1997).
[13] See, for example, A. Ichihara, T. Shirai, and Jörg Eichler, Phys. Rev. A **49**, 1875 (1994); P. H. Mokler and Th. Stöhlker, in *Advances in Atomic, Molecular, and Optical Physics*, edited by B. Bederson and H. Walther (Academic, New York, 1996), Vol. 37, pp. 297–370.
[14] D. Brandt, K. Eggert, and A. Morsch, CERN Report No. AT/94-05, 1994.
[15] T. Chujo *et al.*, Nucl. Instrum. Methods Phys. Res., Sect. A **383**, 409 (1996).
[16] H. F. Krause, E. F. Deveney, N. L. Jones, C. R. Vane, S. Datz, H. Knudsen, P. Grafström, and R. H. Schuch, Nucl. Instrum. Methods Phys. Res., Sect. B **124**, 128 (1997).
[17] S. Datz, H. F. Krause, C. R. Vane, H. Knudsen, P. Grafström, and R. H. Schuch, Phys. Rev. Lett. **77**, 2925 (1996); S. Datz, J. R. Beene, P. Grafström, H. Knudsen, H. F. Krause, R. H. Schuch, and C. R. Vane, Phys. Rev. Lett. **79**, 3355 (1997).
[18] W. L. Wiese and G. A. Martin, in *Physics Vade Mecum*, edited by H. L. Anderson (AIP, New York, 1989), p. 99.
[19] Th. Stöhlker *et al.*, Phys. Lett. A **238**, 43 (1998).